Taylor & Francis
Taylor & Francis Group

Check for updates

Synthesis of new carbon material produced from human hair and its evaluation as electrochemical supercapacitor

Derya Bal Altuntaş [a], Sema Aslan [b], Yeşim Akyol [c], and Vagif Nevruzoğlu [c]

aDepartment of Bioengineering, Faculty of Engineering, Recep Tayyip Erdogan University, Rize, Turkey; bDepartment of Chemistry, Faculty of Science, Mugla Sitki Kocman University, Muğla, Turkey; cDepartment of Energy Systems Engineering, Faculty of Engineering, Recep Tayyip Erdogan University, Rize, Turkey

ABSTRACT

In this study, carbon material similar to graphene structure (GLS) was prepared from graphite and the carbonization of Turkish human hair fibers (HHC) and utilized for the modification of electrode to evaluate the supercapacitance performance. Electrochemical characterization of the HHC-based GLS (HHC-GLS) modified electrodes have been carried out with cyclic voltammetry and electrochemical impedance spectroscopy. The morphology and chemical composition of the resultant GLSs were characterized by scanning electron microscopy, X-Ray diffraction spectroscopy, Raman and Fourier Transform infrared spectroscopy analysis. HHC-GLS displayed a good electrochemical activity than the graphite sourced graphene and possess very similar morphological properties with commercial graphene. Carbonization of the waste hair was carried out at 280°C to improve the pore structure as the first step of GLS synthesis. HHC-GLS modified electrode exhibited the best electrochemical activity and utilized as a charge storage device. The best specific capacitance value was found to be 139.00 F g^{-1} in 6.00 M $KOH_{(aq)}$ at a scan rate of 100.00 mV s^{-1} and good stability over 500 cycles. Whereas an energy density of 19.3 Wh kg^{-1} and power density of 6.95 kW kg^{-1} were obtained from the electrode when operated in the voltage range from −1.00 to 0.00 V. This work offers a new approach to human hair waste management in terms of promising green energy applications. This study was patented by the Turkish Patent and Trademark Office (Turkish Patent Institute Application Number: (2019/22841)).

Introduction

Divergent renewable energy systems have been invented in the last decades (Kong et al. 2019). The batteries are an attainable branch of these systems. Although the most common type of battery is Li-ion battery, it suffers from the depletion of Lithium resources, therefore increase in its cost. Since the conventional batteries show identical drawbacks (low lifetime, toxicity, high cost an explosion risk, etc.) efforts on the researches for the alternative type of batteries (Li-Sulfur, Al-Air battery, etc.) and capacitors have been motivated. (Yanik et al. 2017) Supercapacitors show infinite charging-discharging cycles, whereas batteries lose their chargeability after a number of cycles (Wang et al. 2014) Supercapacitors are classified as pseudocapacitors, electrochemical double-layer capacitors (EDLC), and hybrid capacitors. (Obreja 2008) EDLCs store charge by the non-faradaic mechanism, in which physical processes dominate the distribution of charges on the surfaces (Huggins 2000). Hence, the conventional capacitors have low energy densities the materials need to be improved to achieve higher power densities and meet the energy performance of batteries. Scientific interest is

---

CONTACT Derya Bal Altuntaş ✉ derya.balaltuntas@erdogan.edu.tr 🏛 Department of Energy Systems Engineering, Faculty of Engineering, Recep Tayyip Erdogan University, Rize, Turkey

focused on the application of the carbon-based materials on the development of novel energy production and storage devices have attracted much attention due to the high costs of commercially available noble metal catalysts. Divergent forms of carbon-based materials are classified as electrochemical double-layer capacitors (EDLC). (Ahmed et al. 2017b)

Graphene possesses a substantial scenario in improving the technical performance of a wide range of energy applications (Cossutta et al. 2020). Besides graphene comes into prominence with wide specific surface area (2630.00 m^2 g^{-1}), high electrical conductivity and chemical stability, as well as excellent mechanical, thermal, and optical properties, has become popular especially for supercapacitors. (Korkmaz and Kariper 2020) Seamless graphene/nanotubes are constructed and integrated into textile electrodes as a stretchable supercapacitor (Liu et al. 2020). Also, hydrophilic graphene/graphene oxide nano-sheets produced for supercapacitor electrode (Tian et al. 2019). Recently performance of graphene was compared to the activated carbon in terms of life-cycle in the environment and graphene supercapacitors are indicated as the least impacting material. (Cossutta et al. 2020) Recovery of waste materials or lowering the life cycle of the energy materials is possible with the management of the source material. Different types of carbon-based catalysts from waste recovery reported up to date with their excellent improving effect on the reactions compared to the commercial products. (Anthonysamy et al. 2018) Graphene is one of the most famous member of these carbon-based materials which has been produced from divergent types of biomass. Here it is the first time that graphene is produced from human hair waste in Turkey and utilized in a supercapacitor.

Conventional graphene production methods can be sorted as, chemical reduction in hydrazine (Liu et al. 2010), micromechanical cleavage (Novoselov1 et al. 2004), microwave exfoliation of GO (MEGO), chemical vapor deposition (CVD) (Yang et al. 2015), laser scribing (LSG) (El-Kady et al. 2012), and mechanical ablation (Janowska et al. 2012), one-step hydrogen annealing (HAG) (Yang et al. 2017), epitaxial growth (Berger et al. 2006), and so on. Among them, high-quality graphene is produced by CVD and epitaxial growth, but the process is very complex, working conditions are harsh and relatively high in cost so these disadvantages prevent their applicability. According to the literature, the most hopeful and environmentally friendly method for large-scale production of graphene is the reduction of graphene oxide from carbon sources (Tian et al. 2019). Much of the abovementioned methods are based on using fossil fuel derivatives (Zhang, Gu, and Zhao 2013). However, the usage of different carbon sources affects the conductivity of graphene due to final chemical composition or structural defects. Compared to the petroleum originated resins, biomass (waste)-based production ways human hair (Ahmed et al. 2017a), plants (Gnerlich et al. 2015), coal (Huang et al. 2016), dung (Gupta, Aneja, and Rana 2016), etc., for graphene are promoting with the advantages of low cost and environmental friendliness. (Baltenneck et al. 2000) Environmental pollution is the common problem of the earth's livings and rapidly increasing due to population growth and urbanization. Waste management territories of the G20 decree in Turkey have taken the most important agenda of including hair wastes. As being a valuable carbon source for graphene production, human hair wastes are disposed of by burning them. During the burning, the high N content of human hair causes the release of some toxic gases as a result of the combustion process and triggers global warming. (Gupta 2014) Besides, the organic properties of oily hair follicules cause microbiological health problems at waste collection centers. Until now various carbon based materials were synthesized from human hair and it is especially a great activated charcoal source with the disulfide bonds. (Hearle 2000) Qian et al. reported human hair-derived carbon flakes for electrochemical supercapacitors (Qian et al. 2014), human hair-derived N and S doped porous carbon materials for gas adsorption (Zhao et al. 2015) or supercapacitors and supercapacitor applications reported. (Si et al. 2013) needlelike MnO_2/activated carbon nanocomposites derived from human hair for supercapacitors are also reported. (Deng et al. 2015) In this study, we demonstrate the synthesis of heteroatom-doped GLS via the carbonization of human hair. (Zhao et al. 2015) Gopalakrishnan et al. reported heteroatom-doped few-layer graphene-like microporous carbon nanosheets from biomass for high-capacitance supercapacitors. (Gopalakrishnan, Kong, and Badhulika 2019) There have been reported other carbon-based materials utilized supercapacitors such as carbide derived carbon fiber-

electrodes with 120 F g^{-1} Csp value (Gao et al. 2012), microporous carbon using another study with 92 F g^{-1} (Ania et al. 2009), exohedral carbon structures (20–100 F g^{-1}) (Frackowiak et al. 2001), oxidized MWCNTs with 102 F g^{-1} (Niu et al. 1997) or graphene-based materials with 94 F g^{-1} Csp value. (Yu et al. 2010) These studies exhibited only moderate supercapacitance performances lower than presented study. Recently (Zhao et al. 2020) reduced graphene oxides on human hair fibers and utilized this flexible material as a supercapacitor successfully. Differently, here we directly GLSs from human hair fibers. The novelty of this study is that a graphene-like material is synthesized from human hair and this material is successful in supercapacitor modification. We firstly report that hair constituents trigger the mesoporous structure production that enhances the electrocapacitive ability of electrode. (Zhang et al. 2012) When the human hair is heated, the sulfur pressure in the medulla (the innermost layer of the hair) increases and causes small bangs due to its anisotropic properties (Bal Altuntaş et al. 2020). Thus, it shows a porous structure in a short time at low temperatures that give biocompatibility features to the hair as a carbon source. In the present study, we succeeded the production of a very valuable catalyst from a waste human hair biomass. GLS has been derived from graphite and human hair employing a Modified Hummers method. Since HHC-GLS exhibited the best electrochemical activity and utilized as a charge storage device. Besides, according to structural and morphological characterization results, HHC-GLS displayed very similar morphological properties with commercial graphene. Supercapacitance properties of HHC-GLS were evaluated and the Csp performance was found to be convenient after 1000 charge-discharge cycles. It can be concluded that the human hair is a very promising raw material for the GLS synthesis for the supercapacitor intended applications.

Experimental

Apparatus

Graphite powder and mineral oil were purchased from Sigma-Aldrich. Potassium dihydrogen phosphate (KH$_2$PO$_4$) potassium chloride (KCl), potassium hydroxide (KOH) were obtained from (Merck). Hydrogen peroxide (H$_2$O$_2$) and sulfuric acid (H$_2$SO$_4$) were obtained from Sigma Aldrich, sodium nitrate (NaNO$_3$) and potassium permanganate (KMnO$_4$), hydrazine (80%), ammonia (NH$_3$) were obtained from Merck. Structural and morphological characterizations were performed by scanning electron microscopy (SEM), X-Ray diffraction spectroscopy (XRD), raman, and fourier transform infrared (FTIR) spectroscopy analysis. Crystallographic characterization of metal impregnated active carbon was made with Rigaku Smart XRD spectrometer. First, to ensure the conductivity of all samples, the surface of the samples (Quorum, SC-7620) was coated with gold (Au) at 99% purity in argon gas medium for about 150.00 sec. Then, in the scanning electron microscope (SEM) (JEOL Brand JSM 6610 model), the surface morphology of the samples was examined with 10.00 kV acceleration voltage in a vacuum environment. Witec Alpha 300 R was used for Micro Raman spectroscopy analyses. Autolab PGSTAT 204 potentiostat/galvanostat (Metrohm Autolab B.V.) electrochemical measurement system is driven by NOVA 2.1.4 software was used.

Preparation of activated carbon

The human hair waste used in the study was uncolored and unscented. It was washed with distilled water to cleanse it from dirt and dust, then dried. In this study, the chemical activation process wasn't used in the carbonization processes. Heat treatment was applied as 280.00 $^{\circ}$C for 40.00 minutes in air free, inert (argon) environment. During this process, human hair mass which loses the elasticity was grinded mechanically and the magnitudes of examples downsized to 10 μM in length. At last, the degassing process was performed by waiting for the charred material for 24.00 hours under 2.00×10^{-3} Torr pressure and 110.00°C temperature value.

Electrode preparation and electrochemical measurements

Autolab PGSTAT 204 potentiostat/galvanostat (Metrohm Autolab B.V.) workstation was used for the electrochemical measurements. Three electrodes system was composed of a platinum electrode (CH Instruments Inc. CHI 111) as the counter, Ag/AgCl (containing 3.00 M KCl, CHI115) as reference electrode and a composite working electrode immersed in 3.00 mL of 6.00 M $KOH_{(aq)}$ electrolyte. GLS modified composite electrode was prepared by mixing 70:30 (w/w %) graphite powder/mineral oil and an optimized amount of GLS. Cyclic voltammetry (CV) (scan rate from 5.00 to 100.00 mV s^{-1}) and differential pulse voltammetry (DPV) measurements were recorded in the 6.00 M $KOH_{(aq)}$ solution using the potential range of −1.00–0.00 V. Electrochemical impedance spectroscopy (EIS) was measured in a frequency range of 10^{-1} to 10^4 Hz in 3.00 mL of 6.00 M $KOH_{(aq)}$ solution. The modified working electrode was prepared as reported in our previous studies (Altuntaş et al. 2017). The electrode surface was renewed and polished before every measurement and all experiments were repeated three times. Double distilled water was used for all of the rinsings, dilutions, and preparation of the solutions. Csp was calculated according to the following equation (Equation (1)). Galvanostatic charge discharge cycles were carried out for the different scan rates applied.

$$C_S = \frac{1}{mVS} \ I(V)dV \tag{1}$$

Cs; specific capacitance, I; current, S; scan rate, m; the mass of the AC on the electrode and ΔV; applied potential range, t is time (h) respectively. The specific energy (E) (Wh kg^{-1}) (Equation (2)) and specific power (P) (W kg^{-1}) densities were calculated from Equation (3). (Mu et al. 2017)

$$E = \frac{1}{2} \left(\frac{1}{3.6} \right) (V^2) \tag{2}$$

$$P = \frac{E}{t} \tag{3}$$

Results and discussion

Synthesis and characterization of new carbon material

There have been several attempts for the production of graphene so far (Wu et al. 2020). Here, we present a modified Hummers method that uses activated carbon produced from waste hair as initiator material instead of graphite. Detailed synthesis and the operational parameters are given in our previous report (Altuntas, Tepeli, and Anik 2016). At the first stage, the graphene oxide synthesis is indicated by the color transition of the mixture from black to brown. At the second stage, graphene oxide was reduced into the GLS which was utilized for the electrode modifications. The schematic presentation of the study was given in Figure 1. SEM images of the graphene from graphite and, HHC-GLS sample are given, respectively, in Figure 2.

Raman spectrums of graphene from graphite and HHC-GLS are given in Figure 3. Here in G and D peaks are defined in the Raman spectra of carbon structures. (Wang, Alsmeyer, and McCreery 1990) D peak is produced by hybrid sp^3 weave vibrations and G peak is produced by sp^2 carbon weave vibrations. The density of the G Peak (I_G) refers to regular crystal structures, while the density of the D Peak (I_D) refers to irregular crystal structures. However, the ratio between the peaks also determines the oxygen to carbon ratio in the graphene structure (O/C). D and G peaks were determined at 1347.00 cm^{-1} and 1565.00 cm^{-1} respectively from Raman measurements. Separation in the peaks was clearly observed in HHC-GLS. By calculating the I_D/I_G ratio, information about the crystal structure of the sample is obtained. (Tuinstra and Koenig 1970) As can be seen from the figure, the I_D/I_G ratio is less than 1 in the graphene structure produced. This result shows that instead of the reduction
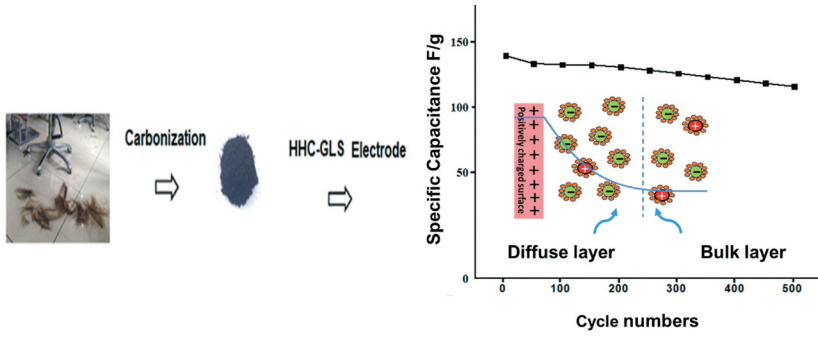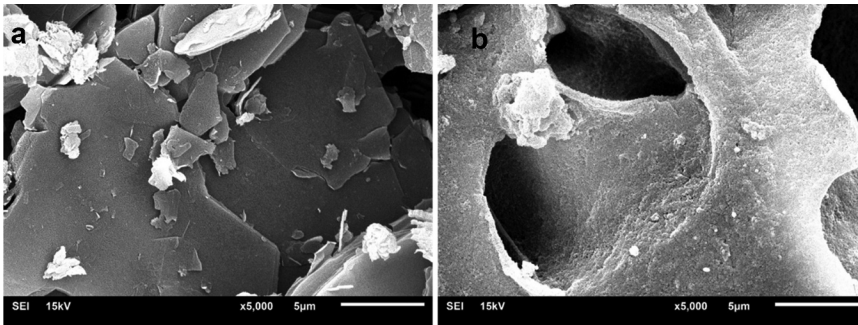
Figure 1. Schematic presentation of the work.

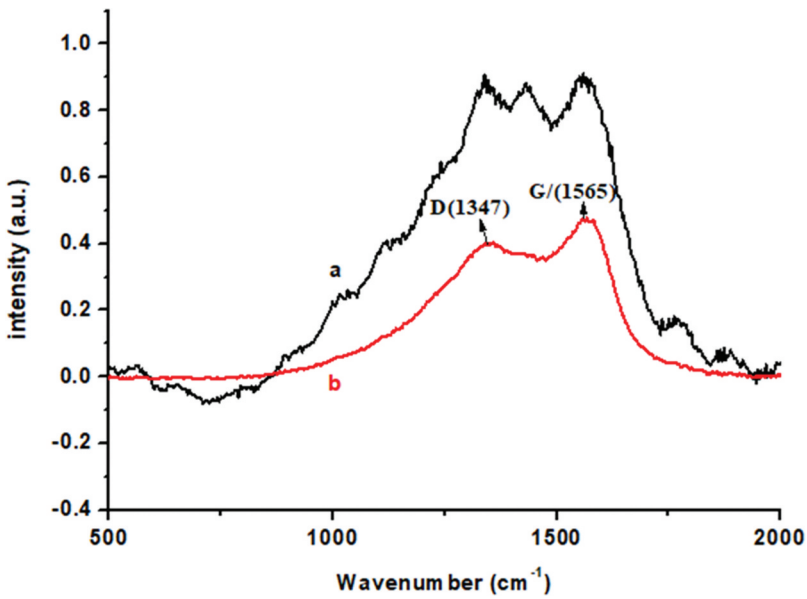**Figure 2.** SEM images of a) graphene from graphite b) HHC-GLS samples.

Figure 3. Raman spectrums of a) graphene from graphite and b) HHC-GLS.

reaction, functional spherical groups (COOH, CO, OH, H_2O) have formed new sp^2 carbon networks and increased the amount of regular structures.
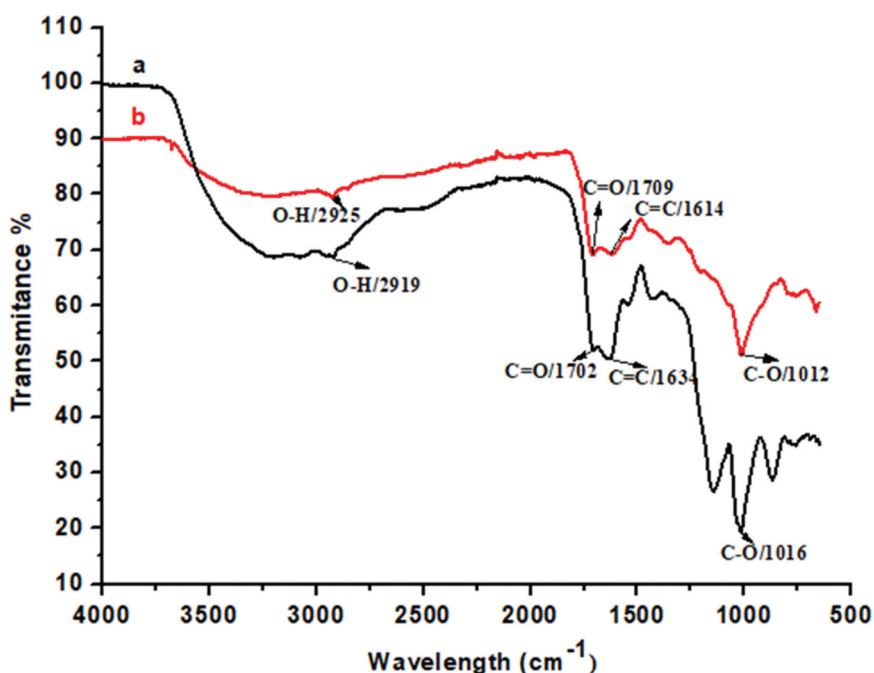
Figure 4. FT-IR spectra of a) graphite derived graphene and b) HHC-GLS.

Figure 4 shows the FT-IR spectrum of graphite derived graphene (Figure 4a) and HHC-GLS (Figure 4b). C = O stresses belonging to carboxyl groups were observed at 1702.00 cm^{-1} and O-H stresses belonging to hydroxyl groups were observed at 2919.00 cm^{-1}. C-O stress of alkoxy groups gives a wide peak at 1016.00 cm^{-1}. These results show that waste human hair was converted into graphene like nanostructure due to the changes at the abovementioned peaks. Some of the peaks show different intensities but the wavelengths show good correlation.

As it is known, graphene has a two-dimensional hexagonal crystal structure (hexogonal) consisting of hexagonal cells. The fact that the graphene has a two-dimensional crystal structure allows it to be used in wider technology areas. Another point that makes this crystal structure interesting is that its reverse weave is also hexagonal. XRD analysis is used to investigate the interlayer changes and crystal structure properties of the material. In Figure 5, XRD spectrum of graphene obtained as a result of reduction reaction of waste human hair is given. As can be seen, all reflection peaks exhibited in the spectrum have sharp character and reflections originating from amorphous structure are not found. This result shows that the objective GLS has been successfully synthesized from waste hair by using the modified Hummers method. Preferred orientation appears to be $2\theta = 26°$ in the given XRD spectrum. This reflection peak is the characteristic peak of the hexagonal graphene structure and is caused by its (002) plane. However, the reflection in the $2\theta = 10°$ value of spectrum also originates from the (002) plane and belongs to graphene oxide as reported in the studies (Asgar et al. 2018). The crystal size and number of layers of the graphene structure was calculated by the Scherrer equation and found as 25 nm and 74. However, a series of low-intensity clustered reflections appear between $2\theta = 20° -30°$ of the spectrum. These reflections may be attributed to metal oxide phases (such as NaO, KO) formed as a result of the settled chemicals in the crystal structure, used in the modification process.

Electrochemical measurements of HHC-GLS electrode

Electrochemical measurements carried out for the optimization of HHC-GLS amount and characterization of the developed supercapacitor electrode. DPV was used for the determination of the
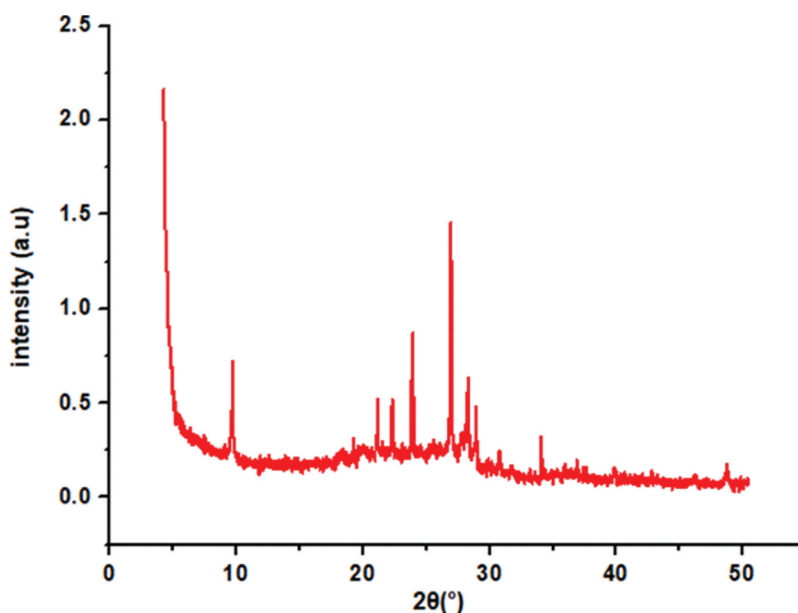
Figure 5. XRD results of HHC-GLS.

optimum amount of GLS in electrode modification. The comparison of voltammograms obtained for different amounts of HHC-GLS electrode (1.00%, 2.00%, 6.00%, 8.00%, and 10.00% by mass of the electroactive material). The optimum amount of HHC-GLS was determined as 8.00%.

CV is generally used for the analysis of the electrochemical transfer mechanism on the electrode surface. Here the case is the examination of the charge transfer mechanism between the electrode surface and the electrolyte. To explain the charge transfer rate all of the HHC-GLS modified electrode was measured for different scan rates of 5.00 (a), 20.00 (b), 50.00 (c), and 100.00 (d) mV s^{-1} in Figure 6.

Each of the voltammograms are evaluated by the calculation of the peak areas of the completed cycles. These areas are divided into the effective electrochemical active mass of the corresponding electrode in order to achieve Csp value. All of the Csp, E and P values of each scan rate are given in Table 1. According to the knowledge given in the literature observed values are at an attainable level of those reported carbon-related EDLCs. (Béguin et al. 2014; Frackowiak et al. 2001)

Cyclic voltammograms of graphite-based (Fig. 7Aa) and HHC-GLSs (Fig. 7Ab) were performed at the scan rate of 100.00 mV s^{-1}. Subsequently, electrochemical activity of the GLS modified electrodes was examined by impedimetric analysis. Obtained impedance spectrums exhibited two components: semicircle part and linear part. These are known as Nyquist plots and found to be compatible with the Warburg model. In Figure 7b it can be seen that semicircle of the HHC-GLS modified electrode show differences from graphite derived graphene. Warburg model says that if the semicircle of the plot gets larger due to the electrons face with a resistance impedance gets higher. Here HHC-GLS modified electrode shows the smallest semicircle part and the slope after semicircle is higher than graphite derived graphene modified electrode. This situation is explained as the charge transfer capability of the electrode is the best for HHC-GLS modified electrode. To sum up, HHC-GLS modified electrode has shown the best electrochemical behavior and this is attributed to its unique surface properties and electroactive cavities.

Typically, these exohedral carbons exhibit SBET of only 300–500 m^2 g^{-1}, and correspondingly, they show usually a moderate Csp of only 20–100 Fg^{-1}. Yet, the highly graphitic nature and external surface area make these materials suitable for fast charge and discharge applications. (McDonough et al. 2012)
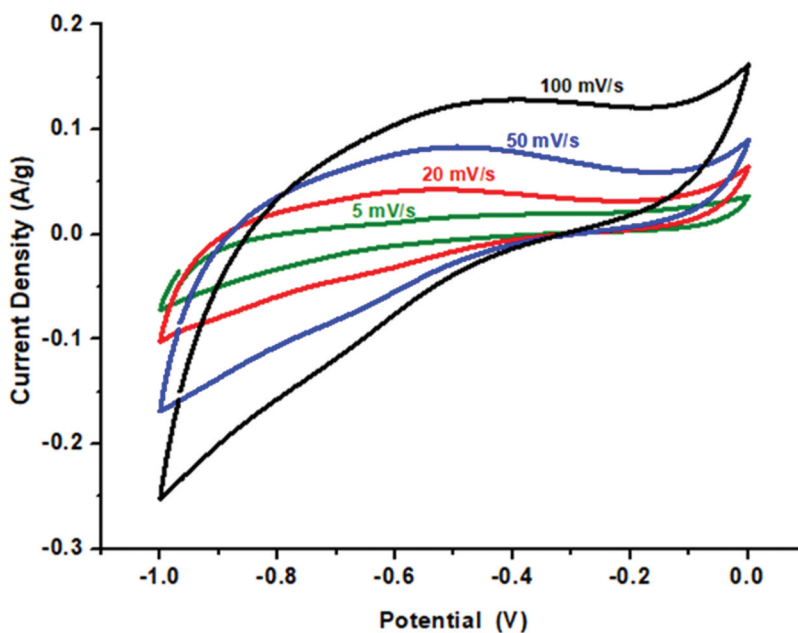
Figure 6. Cyclic voltammograms of HHC-GLSs at scan rate from a 5.00 mV s^{-1} (b) 20.00 mV s^{-1} (c) 50.00 mV s^{-1} (d)100.00 mV s^{-1}.

Table 1. Specific capacitance, energy, and power densities for each scan rate.

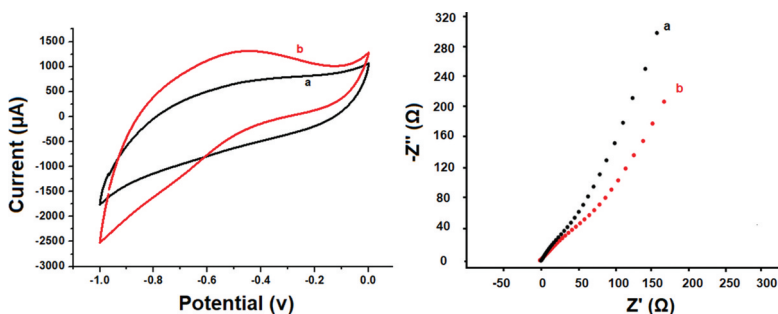| Scan rate/mV s^{-1}	Csp/F g^{-1}	E/Wh kg^{-1}	P/kW kg^{-1}
5	22.74	3.16	1.14
20	51.57	7.17	2.58
50	93.67	13.02	4.69
100	139.22	19.35	6.97

Figure 7. a Cyclic voltammograms of a) graphite-based and b) HHC-GLSs at the scan rate of 100.00 mVs^{-1}. b Nyquist EIS plots were obtained in a frequency range of 10^{-1} to 10^4 Hz in the 6.00 M KOH$_{(aq)}$ solution.

Later studies show moderate intrinsic Csp (18–137 F g^{-1}) for single-wall and multi-wall CNTs in 6.00 M KOH$_{(aq)}$ aqueous electrolyte (Frackowiak et al. 2001).

Figure 8a shows the charge/discharge cycling behavior of HHC-GLS modified electrode at a constant scan rate of 100.00 mV s^{-1} between −1.00 and 0.00 V potential values for 500 cycles. Figure 8b illustrates the long-term Csp stability test of the HHC-GLS modified electrode. The best Csp value was observed as 139.00 F g^{-1}, E was obtained as 19.30 Wh kg^{-1} and P was 6.95 kW kg^{-1} in 6.00 M KOH$_{(aq)}$ solution, at a scan rate of 100.00 mV s^{-1} and exhibited good stability over 500 cycles. The Csp
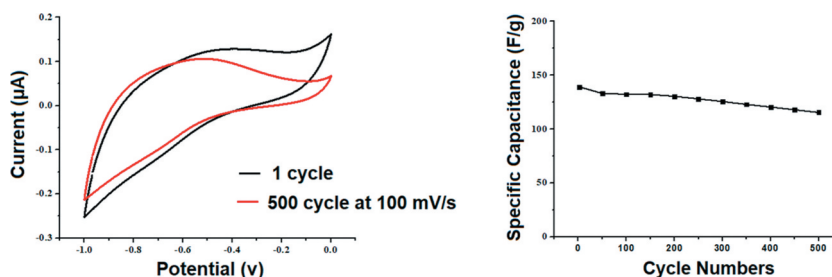
Figure 8. Cyclic stability of HHC-GLS modified electrode a shows the comparison of the 500th CV cycle with the 1st CV cycle at 100.00 mV s^{-1} b Change of the Csp values for 500 cycles at 100.00 mVs^{-1}.

values were stable over the 500 cycles and about 121.00% of the initial Csp was still maintained, suggesting that the HHC-GLS modified electrode has superior charge/discharge ability.

Conclusions

According to our previous studies, activated charcoal synthesized using waste human hair is a very useful electrode material. In this study, graphene-like carbon material, which uses this material as a source, was synthesized successfully. The work done up to this stage has not yet been reported in the literature. The synthesized HHC-GLS was used in carbon paste electrode modification as a composite nanomaterial. The Csp value of the developed electrode was found to be 139.00 F g^{-1} at the scan rate of 100.00 mV s^{-1}. This result is quite remarkable among carbon-based supercapacitors for HHC-GLS material, whose performance has been tried for the first time in such a study. Also, the developed electrode has stayed stable even after 500 cycles of charge/discharge. The study presented in this sense shows the hair waste is how useful as a carbon source and that it is suitable for use in studies for clean energy production. It has a great potential for the future fuel cell, battery, or sensor development researches.

Notes on contributors

Derya Bal Altuntaş accepted her license, MSc. and Ph.D. degrees from the Chemistry department. Completed her Ph.D. thesis on sensors. Currently is an Asst. Prof. Dr. in Bioengineering department and studying biosensors.

Sema Aslan accepted her license, MSc. and Ph.D. degrees from the Chemistry department (Electroanalytic chemistry). Completed her Ph.D. thesis on microbial fuel cells. Currently is a Research Assist. in the Chemistry department and studying renewable and green energy productions.

Yeşim Akyol accepted her license Energy Systems Engineering department. Currently works in the energy sector.

Vagif Nevruzoğlu accepted his license Physics engineering and Ph.D. degrees from the Physics Institute, Completed his Ph.D. thesis Alternative Energy Sources. Currently is a Prof. Dr. in Energy Systems Engineering department and studying energy.

ORCID

Derya Bal Altuntaş 🆔 http://orcid.org/0000-0001-6544-6271
Sema Aslan 🆔 http://orcid.org/0000-0001-9796-7311
Yeşim Akyol 🆔 http://orcid.org/0000-0003-3918-7477
Vagif Nevruzoğlu 🆔 http://orcid.org/0000-0002-8758-4760

References

Ahmed, M. J., M. A. Islam, M. Asif, and B. H. Hameed. 2017a. Human hair-derived high surface area porous carbon material for the adsorption isotherm and kinetics of tetracycline antibiotics. *Bioresource Technology* 243:778–84. doi:10.1016/j.biortech.2017.06.174.

Ahmed, S., Y. Bhat, M. Rafat, and S. A. Hashmi. 2017b. Low temperature thermal exfoliation of graphene oxide for high performance supercapacitor. *Journal of Materials Science and Surface Engineering Science* 5:571–76. doi:10.jmsse/2348-8956/5-3.5.

Altuntaş, D. B., G. Akgül, J. Yanik, and Ü. Anik. 2017. A biochar-modified carbon paste electrode. *Turkish Journal of Chemistry* 41:455–65. doi:10.3906/kim-1610-8.

Altuntas, D. B., Y. Tepeli, and U. Anik. 2016. Graphene-metallic nanocomposites as modifiers in electrochemical glucose biosensor transducers. *2D Materials* (3):1–8. doi:10.1088/2053-1583/3/3/034001.

Ania, C. O., J. Pernak, F. Stefaniak, E. Raymundo-Piñero, and F. Béguin. 2009. Polarization-induced distortion of ions in the pores of carbon electrodes for electrochemical capacitors. *Carbon* 47:3158–66. doi:10.1016/j.carbon.2009.06.054.

Anthonysamy, S. B. I., S. B. Afandi, M. Khavarian, and A. R. B. Mohamed. 2018. A review of carbon-based and non-carbon-based catalyst supports for the selective catalytic reduction of nitric oxide. *Beilstein Journal of Nanotechnology* 9:740–61. doi:10.3762/bjnano.9.68.

Asgar, H., K. M. Deen, U. Riaz, Z. U. Rahman, U. H. Shah, and W. Haider. 2018. Synthesis of graphene via ultra-sonic exfoliation of graphite oxide and its electrochemical characterization. *Materials Chemistry and Physics* 206:7–11. doi:10.1016/j.matchemphys.2017.11.062.

Bal Altuntaş, D., V. Nevruzoğlu, M. Dokumacı, and Ş. Cam. 2020. Synthesis and characterization of activated carbon produced from waste human hair mass using chemical activation. *Carbon Letters* 30 (3):307–13. doi:10.1007/s42823-019-00099-9.

Baltenneck, F., Bernard, J. C. Engström, P. Riekel, C. Leroy, F. Franbourg, and J. Doucet. 2000. Study of the keratinization process in human hair follicle by X-ray microdiffraction. *Cellular and Molecular Biology (Noisy-le-grand)* 46:1017–24. http://www.ncbi.nlm.nih.gov/pubmed/10976881.

Béguin, F., V. Presser, A. Balducci, and E. Frackowiak. 2014. Carbons and electrolytes for advanced supercapacitors. *Advanced Materials* 26:2219–51. doi:10.1002/adma.201304137.

Berger, C., Z. Song, X. Li, X. Wu, N. Brown, C. Naud, D. Mayou, T. Li, J. Hass, A. N. Marchenkov, et al. 2006. Electronic confinement and coherence in patterned epitaxial graphene. *Science* 312:1191–96. doi:10.1126/science.1125925.

Cossutta, M., V. Vretenar, T. A. Centeno, P. Kotrusz, J. McKechnie, and S. J. Pickering. 2020. A comparative life cycle assessment of graphene and activated carbon in a supercapacitor application. *Journal of Cleaner Production Journal* 242:118468. doi:10.1016/j.jclepro.2019.118468.

Deng, D., B. S. Kim, M. Gopiraman, and I. S. Kim. 2015. Needle-like MnO2/activated carbon nanocomposites derived from human hair as versatile electrode materials for supercapacitors. *RSC Advances* 5:81492–98. doi:10.1039/c5ra16624a.

El-Kady, M. F., V. Strong, S. Dubin, and R. B. Kaner. 2012. Laser scribing of high-performance and flexible graphene-based electrochemical capacitors. *Science* 335 (6074):1326–30. doi:10.1126/science.1216744.

Frackowiak, E., K. Jurewicz, S. Delpeux, and F. Béguin. 2001. Nanotubular materials for supercapacitors. *Journal of Power Sources* 97–98:822–25. doi:10.1016/S0378-7753(01)00736-4.

Gao, Y., V. Presser, L. Zhang, J. J. Niu, J. K. McDonough, C. R. Pérez, H. Lin, H. Fong, and Y. Gogotsi. 2012. High power supercapacitor electrodes based on flexible TiC-CDC nano-felts. *Journal of Power Sources* 201:368–75. doi:10.1016/j.jpowsour.2011.10.128.

Gnerlich, M., H. Ben-Yoav, J. N. Culver, D. R. Ketchum, and R. Ghodssi. 2015. Selective deposition of nanostructured ruthenium oxide using tobacco mosaic virus for micro-supercapacitors in solid nafion electrolyte. *Journal of Power Sources Journal* 293:649–56. doi:10.1016/j.jpowsour.2015.05.053.

Gopalakrishnan, A., C. Y. Kong, and S. Badhulika. 2019. Scalable, large-area synthesis of heteroatom-doped few-layer graphene-like microporous carbon nanosheets from biomass for high-capacitance supercapacitors. *New Journal of Chemistry* 43:1186–94. doi:10.1039/c8nj05128c.

Gupta, A. 2014. Human hair "waste" and its utilization: Gaps and possibilities. *Journal of Waste Management* ID 498018:17. doi:10.1155/2014/498018.

Gupta, K. K., K. R. Aneja, and D. Rana. 2016. Current status of cow dung as a bioresource for sustainable development. *Bioresources and Bioprocessing* 3:1–11. doi:10.1186/s40643-016-0105-9.

Hearle, J. W. S. 2000. A critical review of the structural mechanics of wool and hair fibres. *Cellular and Molecular Biology (Noisy-le-grand, France)* 27:123–38.

Huang, G., W. Kang, B. Xing, L. Chen, and C. Zhang. 2016. Oxygen-rich and hierarchical porous carbons prepared from coal based humic acid for supercapacitor electrodes. *Fuel Processing Technology* 142:1–5. doi:10.1016/j.fuproc.2015.09.025.

Huggins, R. A. 2000. Supercapacitors and electrochemical pulse sources. *Solid State Ionics* 134:179–95. doi:10.1016/S0167-2738(00)00725-6.

Janowska, I. A., F. Vigneron, D. Be´gin, O. Ersen, P. Bernhardt, T. Romero, M. J. Ledoux, and C. Pham-Huu. 2012. Mechanical thinning to make few-layer graphene from pencil lead. *Carbon* 50:3106–10. doi:10.1016/j.carbon.2012.02.

Kong, W., M. Zhang, Z. Han, and Q. Zhang. 2019. A theoretical model for the triple phase boundary of solid oxide fuel cell electrospun electrodes. *Applied Sciences* 9:493. doi:10.3390/app9030493.

Korkmaz, S., and A. Kariper. 2020. Graphene and graphene oxide based aerogels: Synthesis, characteristics and super-capacitor applications. *Journal of Energy Storage* 27. doi:101038.doi:10.1016/j.est.2019.101038.

Liu, C., Z. Yu, D. Neff, A. Zhamu, and B. Z. Jang. 2010. Graphene-based supercapacitor with an ultrahigh energy density. *Nano Letters* 10:4863–68. doi:10.1021/nl102661q.

Liu, K., Y. Yao, T. Lv, H. Li, N. Li, Z. Chen, G. Qian, and T. Chen. 2020. Textile-like electrodes of seamless graphene/ nanotubes for wearable and stretchable supercapacitors. *Journal of Power Sources Journal* 446:227355. doi:10.1016/j. jpowsour.2019.227355.

McDonough, J. K., A. I. Frolov, V. Presser, J. Niu, C. H. Miller, T. Ubieto, M. V. Fedorov, and Y. Gogotsi. 2012. Influence of the structure of carbon onions on their electrochemical performance in supercapacitor electrodes. *Carbon* 50:3298–309. doi:10.1016/j.carbon.2011.12.022.

Mu, X., J. Du, Y. Zhang, Z. Liang, H. Wang, B. Huang, J. Y. Zhou, X. Pan, Z. Zhang, and E. Xie. 2017. Construction of hierarchical CNT/rGO-supported MnMoO4 nanosheets on Ni foam for high-performance aqueous hybrid supercapacitors. *ACS Applied Materials & Interfaces* 9:35775–84. doi:10.1021/acsami.7b09005.

Niu, C., E. K. Sichel, R. Hoch, D. Moy, and H. Tennent. 1997. High power electrochemical capacitors based on carbon nanotube electrodes. *Applied Physics Letters* 70:1480–82. doi:10.1063/1.118568.

Novoselov, K. S., A. K. Geim, S. V. Morozov, D. Jiang, Y. Zhang, S. V. Dubonos, I. V. Grigorieva, and A. A. Firsov. 2004. Electric field in atomically thin carbon films. *Science* 306:666–69. doi:10.1126/science.1102896.

Obreja, V. V. N. 2008. On the performance of supercapacitors with electrodes based on carbon nanotubes and carbon activated material-A review. *Physics E: Low-dimensional Systems and Nanostructures* 40:2596–605. doi:10.1016/j. physe.2007.09.044.

Qian, W., F. Sun, Y. Xu, L. Qiu, C. Liu, S. Wang, and F. Yan. 2014. Human hair-derived carbon flakes for electrochemical supercapacitors. *Energy & Environmental Science* 7:379–86. doi:10.1039/c3ee43111h.

Si, W., J. Zhou, S. Zhang, S. Li, W. Xing, and S. Zhuo. 2013. Tunable N-doped or dual N, S-doped activated hydrothermal carbons derived from human hair and glucose for supercapacitor applications. *Electrochimica acta* 107:397–405. doi:10.1016/j.electacta.2013.06.065.

Tian, J., S. Wu, X. Yin, and W. Wu. 2019. Novel preparation of hydrophilic graphene/graphene oxide nanosheets for supercapacitor electrode. *Applied Surface Science Journal* 496:143696. doi:10.1016/j.apsusc.2019.143696.

Tuinstra, F., and J. L. Koenig. 1970. Raman spectrum of graphite. *The Journal of Chemical Physics* 53 (3):1126–30. doi:10.1063/1.1674108.

Wang, Q., J. Yan, Y. Wang, T. Wei, M. Zhang, X. Jing, and Z. Fan. 2014. Three-dimensional flower-like and hierarchical porous carbon materials as high-rate performance electrodes for supercapacitors. *Carbon* 67:119–27. doi:10.1016/j. carbon.2013.09.070.

Wang, Y., D. C. Alsmeyer, and R. L. McCreery. 1990. Raman spectroscopy of carbon materials: structural basis of observed spectra. *Chemistry of Materials* 2:557–63. doi:10.1021/cm00011a018.

Wu, D., C. Wang, M. Wu, Y. Chao, P. He, and J. Ma. 2020. Porous bowl-shaped VS2 nanosheets/graphene composite for high-rate lithium-ion storage. *Journal of Energy Chemistry* 43:24–32. doi:10.1016/j.jechem.2019.08.003.

Yang, H., S. Kannappan, A. S. Pandian, J.-H. Jang, Y. S. Lee, and W. Lu. 2015. Nanoporous graphene materials by lowerature vacuum-assisted thermal process for electrochemical energy storage. *Journal of Power Sources Journal* 284:146–53. doi:10.1016/j.jpowsour.2015.03.015.

Yang, H., S. Kannappan, A. S. Pandian, J.-H. Jang, Y. S. Lee, and W. Lu. 2017. Graphene supercapacitor with both high power and energy density. *Nanotechnology* 28:45401. doi:10.1088/1361-6528/aa8948.

Yanik, M. O., E. A. Yigit, Y. E. Akansu, and E. Sahmetlioglu. 2017. Magnetic conductive polymer-graphene nanocom-posites based supercapacitors for energy storage. *Energy* 138:883–89. doi:10.1016/j.energy.2017.07.022.

Yu, J., J. Tu, F. Zhao, and B. Zeng. 2010. Direct electrochemistry and biocatalysis of glucose oxidase immobilized on magnetic mesoporous carbon. *Journal of Solid State Electrochemistry* 14 (9):1595–600. doi:10.1007/s10008-009-0990-3.

Zhang, L. L., Y. Gu, and X. S. Zhao. 2013. Advanced porous carbon electrodes for electrochemical capacitors. *Journal of Materials Chemistry A* 1:9395–408. doi:10.1039/c3ta11114h.

Zhang, M., B. Gao, Y. Yao, Y. Xue, and M. Inyang. 2012. Synthesis, characterization, and environmental implications of graphene-coated biochar. *Science of the Total Environment* 435–436 (2012):567–72. doi:10.1016/j. scitotenv.2012.07.038.

Zhao, R., Y. Wang, Y. Hasebe, Z. Zhang, and D. Tao. 2020. Determination of glucose using a biosensor based on glucose oxidase immobilized on a molybdenite-decorated glassy carbon electrode. *International Journal of Electrochemical Science* 15:1595–605. doi:10.20964/2020.02.45.

Zhao, Z. Q., P. W. Xiao, L. Zhao, Y. Liu, and B. H. Han. 2015. Human hair-derived nitrogen and sulfur co-doped porous carbon materials for gas adsorption. *RSC Advances* 5 (2015):73980–88. doi:10.1039/c5ra15690d.